Effects of linker sequences on vesicle fusion mediated by lipid-anchored DNA oligonucleotides

Yee-Hung M. Chan, Bettina van Lengerich, and Steven G. Boxer[1]

Department of Chemistry, Stanford University, Stanford, CA 94305-5080

Synthetic lipid–oligonucleotide conjugates inserted into lipid vesicles mediate fusion when one population of vesicles displays the 5′-coupled conjugate and the other the 3′-coupled conjugate, so that anti-parallel hybridization allows the membrane surfaces to come into close proximity. Improved assays show that lipid mixing proceeds more quickly and to a much greater extent than content mixing, suggesting the latter is rate limiting. To test the effect of membrane–membrane spacing on fusion, a series of conjugates was constructed by adding 2–24 noncomplementary bases at the membrane-proximal ends of two complementary sequences. Increasing linker lengths generally resulted in progressively reduced rates and extents of lipid and content mixing, in contrast to higher vesicle docking rates. The relatively flexible, single-stranded DNA linker facilitates docking but allows greater spacing between the vesicles after docking, thus making the transition into fusion less probable, but not preventing it altogether. These experiments demonstrate the utility of DNA as a model system for fusion proteins, where sequence can easily be modified to systematically probe the effect of distance between bilayers in the fusion reaction.

DNA machine | synthetic biology

Fig. 1. Comparison of hypothesized docking conformations between membranes presenting (*A*) SNARE proteins (adapted from ref. 13) and (*B*) complementary membrane-anchored DNA in the appropriate orientations. The dimensions of the SNARE complex and a 24-mer hybridized DNA are roughly to scale.

Fusion of lipid membranes plays a central role in many biological processes. For example, in the case of synaptic transmission, the reaction is tightly regulated by a number of proteins of which the SNAREs [soluble *N*-ethylmaleimide sensitive factor (NSF) attachment protein receptors] have been shown to play a crucial role (1–3). *In vitro* studies have demonstrated the sufficiency of SNAREs to mediate fusion when reconstituted into a number of model systems, including free-standing lipid vesicles (4–7), supported lipid bilayers (8–10), and tethered vesicles (11). Generally these studies suggest that SNAREs are able to bring two membranes into close apposition by forming a *trans* complex in a docking reaction which is highly energetically favorable (12). This is illustrated in Fig. 1*A*, which is based on the x-ray structures of the soluble domains of SNARE proteins in complex (13). Several steps along the mechanism to achieve membrane fusion following this basic docking step have been proposed, and some of these are illustrated in Fig. 2, which also serves to illustrate assays commonly used to assess their role. In this step-wise mechanism, the bilayers first dock, then adopt an intermediate, hemifused state in which the outer leaflets have merged, but the inner leaflets and contents remain distinct. A transition into full fusion then involves mixing of both leaflets and content exchange.

Despite substantial research on the role of SNARE proteins in the fusion process, many questions remain regarding the physical mechanism. Studies using simpler model systems can provide insight into the fundamental mechanisms of the rearrangement of bilayers and lead to a better understanding of the biological process (14, 15). We have prepared a series of DNA-lipid conjugates in which DNA oligonucleotides replace the lipid head group, thereby allowing sequence-specific hybridization to bring soft membrane surfaces into close proximity. In the first generations of these conjugates, the DNA was coupled
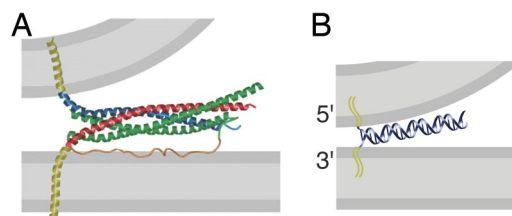
to the lipid anchor at its 5′-end and used to sequence-specifically tether vesicles to supported bilayer surfaces as illustrated in Fig. 3*A* where 5′-β and 5′-β′ represent the single stranded DNA and its complement, respectively. Individual tethered vesicles can be directly visualized by fluorescence microscopy; they are observed to diffuse in a plane parallel to the supported bilayer (16–19) and can be manipulated by external electrical fields and hydrodynamic flow (20). Many collisions between tethered vesicles have been observed, and absent any mediating agent, the vesicles show no tendency to stick to each other or fuse. However, by initially tethering different populations of vesicles to different regions of the supported bilayer, docking reactions between partner vesicles displaying a second complementary sequence (5′-α and 5′-α′ in Fig. 3*B*) could be observed and quantified on the level of individual vesicles (21). The probability of docking upon collision, P_{dock}, showed the following trends: (*i*) a roughly quadratic dependence of P_{dock} on the number density of oligonucleotides on the vesicle docking partners; (*ii*) much more efficient docking for complementary 5′-Poly T / 5′-Poly A* 24-mer sequences than for 24-mer sequences requiring full overlap for hybridization; and (*iii*) a strong increase in the efficiency of docking upon increasing the length of the oligonucleotides by introducing a polyT spacer at the membrane proximal ends. These results were rationalized using a simple geometric model in which P_{dock} was related to the probability of the intersection between cylinders representing 5′-α and 5′-α′ diffusing on the surfaces of colliding vesicles, which are also diffusing. While vesicle co-localization was taken as a measure of docking, in no case was lipid mixing observed. This result was

Fig. 2. Possible stages in DNA-mediated fusion of a pair of lipid vesicles. Separately labeled vesicles present complementary oligomers of DNA coupled to the membrane surface at the 5′- and the 3′-ends. Upon mixing, hybridization of the DNA docks the vesicles together (measured by vesicle co-localization), bringing them into close apposition, followed by a transition to hemifusion that allows mixing of the outer leaflet lipids of the membranes (measured by FRET or FRET dequenching between dye-labeled lipids). Full fusion is achieved when both leaflets merge and contents exchange (measured by observing the onset of fluorescence from $Tb(DPA)^{3+}$ when Tb^{+3} in one vesicle mixes with DPA in another). Note that two DNA-lipid conjugates are shown hybridizing for purposes of illustration, but the actual number required at each step is not known.

Fig. 4. Synthetic method for the lipid phosphoramidite for use as the terminal ''base'' on a DNA-synthesizer (23).

explained by the orientation of the hybridization reaction, in which the resulting duplex is expected to keep the vesicle surfaces physically separated by approximately 8–10 nm for a 24 base docking hybrid as illustrated in Fig. 3*B*.

Inspection of the proposed model for SNARE-mediated fusion in Fig. 1*A* (13) suggests that DNA hybridization might model this process if the orientation of the DNA-lipid conjugates on the reacting vesicles was 5′- and 3′-, rather than both being 5′-. This similarity is illustrated in Fig. 1*B* and in the assays illustrated in Fig. 2. To achieve both couplings, an improved and quite general synthetic route was developed (22) (see Fig. 4 and the *Materials and Methods*). Indeed in bulk assays (vesicles mixed in solution), preliminary data demonstrating both lipid and content mixing were reported (22). As with the docking experiments (12), we found a strong dependence of the kinetics observed by both assays on the number density and sequence of DNA. In particular, for the same number density and lipid composition, 5′-Poly T / 3′-Poly A 24-mers gave a much higher

yield of lipid and content mixing than a fully overlapping complementary sequence pair (22). Related results have been reported using more complex, double cholesterol-anchored-DNA conjugates (23, 24) [singly anchored cholesterol-DNA conjugates, which have been proposed for drug delivery purposes (25), partition only transiently to lipid bilayers or vesicles in contrast to the anchor shown in Fig. 4]. The great advantage of using DNA for these measurements is that the sequence can be readily modified and with the single lipid anchor, nonhybridizing polyT linker extensions can be added to probe the effects of physical proximity during fusion. In the following, we report improved and more quantitative assays and focus on the dependence of each step of the proposed fusion mechanism (illustrated in Fig. 2) on the insertion of variable length polyT spacers to the membrane proximal ends of fully complementary DNA sequences.

Results

Comparison of Lipid and Content Mixing Assays. Because of the large number of variables to be considered in any vesicle fusion experiment, we have chosen a set of standard conditions, specified in the *Material and Methods*, which include lipid composition, vesicle concentration, vesicle size, and temperature. Generally, an average number of DNA-lipid conjugates of 50 per vesicle was used ($<n_{DNA}> = 50$) with the exceptions of the controls with no DNA and the experiments involving a mixture of linker-DNA. To limit variability sometimes observed among different batches of vesicles, sets of experiments in which the linker was varied were performed using aliquots of vesicles from the same preparation. In this way, the only variable for most of the experiments is the length of the linker.

Previously, we observed significant nonspecific lipid mixing in control experiments where vesicles contained either no DNA or noncomplementary DNA (22). Here, we used Oregon Green (OG) and Texas Red (TR) dyes instead of NBD and Rhodamine, which decreased the nonspecific lipid mixing to baseline (Fig. 5*B*, orange trace). The reduction in the nonspecific lipid mixing signal allows a more quantitative comparison of the extents of the lipid and content mixing assays (see *Materials and Methods* for details of assays). These results show that the dye-labeled lipids have a nontrivial impact on the mixing assay, and care must be taken when attempting to compare results among experiments using different dyes. Many experiments have shown that lipid and content mixing are strongly affected by the lipid composition of vesicles (15, 23). Indeed, early attempts in our lab to achieve DNA-mediated fusion using vesicles containing only egg-phosphatidylcholine resulted in much lower extents. In other vesicle fusion systems, incorporation of low mole percents of certain lipids had significant effects on vesicle fusion rates related to the intrinsic curvature of the dopant lipid (26).

It is possible that the lipid dyes increase the rate of fusion; this

Fig. 3. Graphical illustrations of DNA-lipid conjugates in the 5′/5′ orientation used to tether vesicles to supported bilayers and allow vesicle docking. (*A*) Vesicles presenting sequence β are tethered to a supported lipid membrane presenting the complementary sequence β'. These tethered vesicles are observed to diffuse in the plane parallel to the supported membrane. Although they collide, they do not exchange lipids or lose contents (20). (*B*) When a complementary pair, α and α', of DNA-lipid conjugates are displayed on separate vesicles, docking is observed upon collisions depending on the number density, sequence and length of the DNA that is displayed (22).
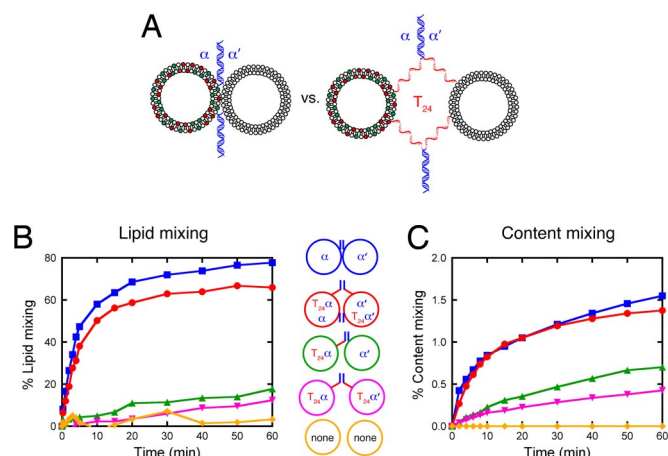
Chan *et al.*

Fig. 5. Fusion mediated by sequence α vs. $T_{24}\alpha$. (*A*) Comparison of the expected docking conformations of vesicles presenting either nonlinker sequences (blue DNA only) and poly T (T_n, shown for $n = 24$) linker sequences (blue and red DNA). Although the single-stranded linker DNA (red) is drawn as a helix, it is likely to be mostly unstructured; two hybrids are shown purpose of illustration only. Representative kinetic traces for (*B*) lipid and (*C*) content mixing collected when two populations of vesicles presenting on average 50 copies of DNA were mixed at equal amounts to a concentration of 2.8 nM in vesicles. Color-coding of the traces is illustrated. Blue: both vesicle populations present only nonlinker sequences $5'$-α/$3'$-α'; Red: both vesicle populations present an average of 50 DNA each (100 total) of nonlinker and linker sequences $5'$-α + $5'$-$T_{24}\alpha$/$3'$-α' + $3'$-$T_{24}\alpha'$; Green: one vesicle population presents nonlinker sequence $5'$-α, and the other presents linker sequence $3'$-$T_{24}\alpha'$; Magenta: both vesicle populations present linker sequences $5'$-$T_{24}\alpha$/ $3'$-$T_{24}\alpha'$; Yellow: vesicles present no DNA (negative control).

may account for the large difference in extent between lipid and content mixing observed. Ideally, both assays should be performed using the exact same lipid composition. However, to date we have been unable to obtain clear results for content mixing assays because of fluorescence interference between the Tb^{3+}-dipicolinic acid (DPA) complex used to monitor content exchange and the included OG and TR leaflet labels (Fig. 2). As a crude alternative that is independent of fluorescence, bulk reactions kinetics were monitored using dynamic light scattering to estimate the average particle size as a function of time (7), and these experiments show little difference when using vesicles with or without the lipid dyes (data not shown). Furthermore, lipid mixing kinetics are similar when OG-DHPE and TR-DHPE are incorporated into the vesicles at 0.5 mol % or 1 mol % each (data not shown).

T_{24} Linker Effects on Docking, Lipid, and Content Mixing. A series of DNA-lipid conjugates was constructed with varying numbers of T bases (T_n linker) added to the membrane proximal end of sequences $5'$-α and $3'$-α' (a nonrepeating, 24-base pair hybridizing sequence requiring full overlap, see Table 1). The sequences of the resulting DNA are as abbreviated as $5'$-$T_n\alpha$ and $3'$-$T_n\alpha'$ (Table 1). When mediating docking, the linker sequences are likely to allow more flexibility in the final conformation of docked vesicles, as depicted for a T_{24} linker in Fig. 5*A*. (Note, these illustrations and those in Fig. 2 show two DNA-lipid conjugates hybridized in cross section, but the actual number of hybrids that lead to lipid and content mixing is not yet known, see *Discussion*). Information on vesicle docking rates in three dimensions was obtained by rapidly diluting dye-labeled vesicles from the fusion reaction mixture and adsorbing them to a glass substrate at various time points (5). These experiments clearly demonstrate that linker sequences $5'$-$T_{24}\alpha$/$3'$-$T_{24}\alpha'$ mediated much faster docking rates than nonlinker sequences $5'$-α/$3'$-α', all other things being equal. This result is consistent with

Table 1. Sequences and coupling orientations of DNA lipids

Name	Sequence
α	lipid-$5'$- TCG ACA CGG AAA TGT TGA ATA CTA $-3'$
α'	$5'$- TAG TAT TCA ACA TTT CCG TGT CGA $-3'$-lipid
$T_{24}\alpha$	lipid-$5'$-TTT TTT TTT TTT TTT TTT TTT TTT TCG ACA CGG AAA TGT TGA ATA CTA $-3'$
$T_{12}\alpha$	lipid-$5'$-TTT TTT TTT TTT TCG ACA CGG AAA TGT TGA ATA CTA $-3'$
$T_6\alpha$	lipid-$5'$-TTT TTT TCG ACA CGG AAA TGT TGA ATA CTA $-3'$
$T_4\alpha$	lipid-$5'$-T TTT TCG ACA CGG AAA TGT TGA ATA CTA $-3'$
$T_2\alpha$	lipid-$5'$-TT TCG ACA CGG AAA TGT TGA ATA CTA $-3'$
$T_{24}\alpha'$	$5'$-TAG TAT TCA ACA TTT CCG TGT CGA TTT TTT TTT TTT TTT TTT TTT TTT-$3'$-lipid

measurements on individual vesicles in two dimensions in the $5'$-/$5'$-orientation (21). While nearly all of the vesicles displaying the $5'$-$T_{24}\alpha$/$3'$-$T_{24}\alpha'$ sequence were colocalized within 5 min, $\approx 70\%$ of vesicles presenting $5'$-α/$3'$-α' docked in the same time period. Interestingly, the orientation of the docking pairs ($5'$-/$5'$-coupled versus $3'$-/$5'$-coupled) did not change the docking rates significantly. Parallel preliminary measurements using tethered vesicles (similar to the situation depicted in Fig. 2*B*, but with the coupling changed to $5'$-α/$3'$-α'), led to the same conclusion.

Bulk vesicle fusion assays with vesicles presenting $5'$-$T_{24}\alpha$/$3'$-$T_{24}\alpha'$ sequences of DNA (Fig. 5*B* and *C*, magenta traces, respectively) showed substantial reductions in both lipid and content mixing kinetics for the linker sequence. Interestingly, similar reductions were observed when the linker sequence was incorporated into only one population of vesicles ($5'$-α/$3'$-$T_{24}\alpha'$, green traces Fig. 5*B* and *C*). When vesicles presenting a mixture of on average 50 copies of linker and 50 copies of nonlinker DNA ($5'$-α + $5'$-$T_{24}\alpha$/$3'$-α' + $3'$-$T_{24}\alpha'$ red traces Fig. 5*B* and *C*), lipid mixing was reduced somewhat compared with vesicles presenting only $5'$-α/$3'$-α' (blue) while content mixing kinetics were similar.

Effect of Shorter Linkers on Lipid and Content Mixing. The dependence of fusion on linker length was investigated by synthesizing a series of DNA-lipid conjugates containing T_2, T_4, T_6, and T_{12} linkers at the membrane proximal end. Because a reduction in fusion is seen even when a linker is incorporated into one vesicle population but not the other, these experiments were performed by reacting one population of vesicles with sequence $3'$-α' (nonlinker) with another population of vesicles presenting sequence $5'$-$T_n\alpha$ (linker DNA, $n = 0–24$). Representative kinetics traces for total lipid mixing (Fig. 6*B*) show similar results for $n = 0$ and $n = 2$, then a systematic reduction in rate and extent as linker length is increased thereafter. Content mixing traces (Fig. 6*C*) show roughly a similar trend, where the apparent difference in final extent from $n = 0$ to $n = 2$ is less than experimental variation.

Discussion

Fusion of vesicles mediated by DNA in the $5'$-/$3'$- orientation is clearly demonstrated by the lipid and content mixing results presented here and previously (22). The earlier work, in addition to that of Stengel *et al.* (23, 24) using a cholesterol-based anchor, found a significant dependence of fusion kinetics on both the number density of DNA on the reacting vesicles as well as sequence (22). The collection of results to date illustrates the utility of having complete sequence control in this model system.

The relationships among the kinetics of docking, lipid mixing, and content mixing are a crucial part of any analysis used to elucidate the mechanisms of fusion. However, comparison between the distinct assays used to monitor these reactions can be complicated. While we attempted to ensure that the comparison
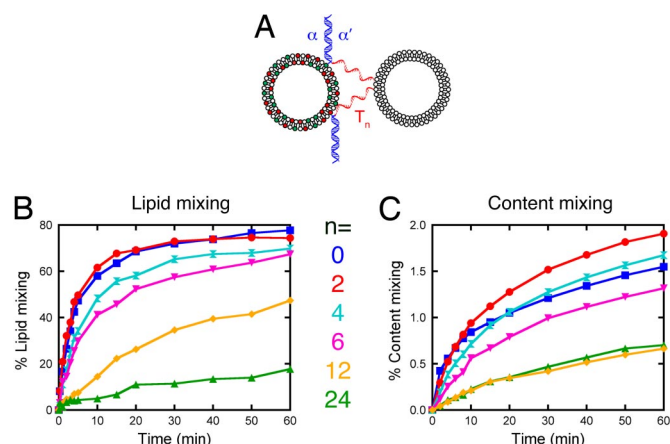
Chan *et al.*

Fig. 6. Effects of linker length on DNA-mediated fusion. (*A*) Expected conformation when a vesicle presenting nonlinker sequences (blue DNA) reacts with one presenting a T_n linker sequence (blue and red DNA). The single-stranded linker DNA is expected to be unstructured; two hybrids are shown purpose of illustration only. Representative kinetic traces for (*B*) lipid and (*C*) content mixing collected when two populations of vesicles presenting an average of 50 copies of DNA were mixed at equal amounts to a concentration of 2.8 nM in vesicles. Color coding of the traces is shown, where the number depicts the length of the oligo-T linker (T_n). In all experiments, the linker sequence $5'-T_n\alpha$ was included in one population of vesicles and the nonlinker sequence $3'-\alpha'$ was included in the other. Blue, $n = 0$; Red, $n = 2$; Green, $n = 4$; Magenta, $n = 6$; Yellow, $n = 12$; Cyan, $n = 24$.

to standards provides meaningful information about fusion extents, for each assay a single value was used to indicate the progression of a complex series of reactions. While this is the standard in kinetic literature and accurately describes reactions with simple mechanisms, in vesicle fusion the exact meanings of percent docking, lipid mixing, and content mixing are not entirely unambiguous. For instance, similar values of percent content mixing could be reached if 30% of vesicles fully exchange all of their contents upon full fusion, or if all vesicles exchange 30% of their contents via flickering fusion pores. Similar considerations exist for lipid mixing assays as well. Another complication is the possibility of multiple docking and fusion events, which cannot be controlled for in these bulk assays. Fusion experiments at the single vesicle level using methods developed to measure tethered vesicle docking in the $5'$-/$5'$-orientation [Fig. 3*B*, (21)] are ongoing. Such assays can control for the number of potential reaction partners and will provide more insight into the issues presented here.

Taking the results at face value, the estimated extents are useful in illustrating broad trends of fusion kinetics. First, a basic comparison can be made between the observed fusion kinetics and those expected for a binary diffusion-limited reaction. By the Einstein-Smolukowski equation, the rate constant for the bimolecular collision of hard spheres of 50 nm diameter in water at 300 K is roughly $k = 7 \times 10^9$ M^{-1}s^{-1}. Using this value and initial concentrations of the vesicles (each 1.4 nM), $t_{1/2} \approx 50$ ms for a diffusion-controlled reaction. To our knowledge, no *in vitro* fusion experiments performed to date with vesicles in bulk solution give docking, lipid, or content mixing kinetics this fast, even using SNAREs or other fusogens. Lipid mixing kinetics for the basic sequence $5'-\alpha/3'-\alpha'$ have $t_{1/2}$ on the order of 5 min based on inspection of the blue time trace in Fig. 5*B*. Thus, there must be a limitation in progressing through one or more of the steps in fusion. Colocalization assays performed in two dimensions using tethered vesicles presenting $5'-\alpha/5'-\alpha'$ (Fig. 3*B*) (21) or in three dimensions using vesicles presenting $5'-\alpha/3'-\alpha'$ (all other factors being equal) indicate a low probability of docking per collision. The extent of docking in bulk assays generally exceeded

the extent of lipid mixing, suggesting a barrier to progressing from docking to lipid mixing.

Content mixing mediated by $5'-\alpha/3'-\alpha'$ proceeds slower and to a far lesser extent than lipid mixing. It is difficult to estimate a $t_{1/2}$ from the blue trace in Fig. 5*C*, as the reaction does not plateau at a final extent by 60 min, which in itself implies a longer $t_{1/2}$ than lipid mixing. Slower kinetics, in addition to the dramatic reduction in extent suggests a significant barrier in progressing from lipid to content mixing, which is consistent with an overall fusion mechanism where content mixing is rate limiting. In this system, content mixing proceeds to less than 2%, while total lipid mixing reaches almost 80%. Control experiments show that contents leak slowly from the vesicles during the fusion reaction, but only ≈ 10% over 1 h. While we did not measure inner leaflet mixing directly, hemifusion would give a maximum of 50–60% total lipid mixing for 50-nm vesicles. These extents, therefore, imply that inner leaflet mixing occurs to a substantially greater degree than content mixing. Comparison of these extents of mixing can be complicated by the fact that lipid mixing experiments use lipid dyes that may change the structure of intermediates along the pathway to fusion. Alternatively, this observation could indicate the formation of an intermediate where the inner leaflets are in contact but aqueous contents remain separate, such as the extended transmonolayer contact stalk (27). Then, inner leaflet lipids could mix if a small lipid-lined pore forms, which may be too small or transient to allow a significant amount of contents to be exchanged.

The addition of linkers of increasing length to the membrane proximal end of the $5'-\alpha/$ $3'-\alpha'$ sequence was found to lead to a general decrease in lipid and content mixing extents. There does not seem to be a critical linker length after which fusion drops dramatically, and fusion remains detectable even with T_{24} linkers. The importance of DNA sequence on fusion has been demonstrated in ref. 22 in which $5'$-Poly T/$3'$-Poly A was found to mediate both lipid and content mixing with faster initial kinetics and to greater extent than the fully overlapping $5'-\alpha/$ $3'-\alpha'$ sequence, all other factors being equal. Interestingly, while the more efficient fusion kinetics for $5'$-Poly T/ $3'$-Poly A (22) parallel the docking efficiency trends found for tethered vesicles (21) and in bulk, the addition of a nonhybridizing linker has opposing effects on docking and fusion. As described in the *Introduction*, the geometric model developed to rationalize the observed trends in docking predicted a substantial increase in docking rate as the linker length is increased, and this prediction was confirmed by the docking rates found for tethered vesicles presenting $5'-\alpha/5'-\alpha'$ or $5'-T_{24}\alpha/5'-T_{24}\alpha'$, where P_{dock} for the latter sequence pair is about one order of magnitude greater than the former (21). Similarly, docking rates measured for vesicles in bulk were much faster for vesicles presenting the linker sequence. Preliminary comparisons of docking mediated by only $5'$-coupled DNA *vs.* by $5'$- and $3'$-coupled DNA reveal similar kinetics, both in the tethered vesicle and in bulk assays. Despite the enhancement of their docking kinetics, vesicles presenting DNA with linkers generally progress to lesser extents of lipid and content mixing, showing that fusion depends on the placement of the recognition sequence with respect to the membrane surface. Indeed, comparison of docking and mixing extents indicates that for linker DNA, docking is unlikely to be the limiting factor in the progression to lipid or content mixing. These results are consistent with recent simulations (28) as well as with experiments performed by Rothman and coworkers (29), who demonstrated the addition of a linker sequence into SNARE proteins can reduce the rates of lipid mixing. Note that docking, whether in the $5'$-/$5'$- or $5'$-/$3'$-orientation, requires only a single DNA hybridization event, while further steps are likely to require multiple (and not necessarily the same number) of hybrids to be formed.

There are several possible reasons for the reduction in fusion rates with linker-DNA. The most likely is that the vesicles are held less tightly together, allowing for greater membrane–membrane distances and, thus, reducing the probability of the lipid rearrangements necessary to transition into hemifusion or full fusion. At an estimated 5–7 Å per base (30), the T_{24} linker would give as much as 12 nm of possible membrane–membrane spacing, while for the shorter linkers the separation would much smaller, only $\approx$1–2 nm maximally for the T_2 linker. The presence of a linker may also reduce the efficient transfer of energy from the hybridization reaction to the membrane anchor in the context of the zippering model proposed for SNARE proteins (31). This concept seems unlikely to us as the free energy liberated by hybridization is rapidly dissipated; rather it seems that the local tension enforced between the membrane surfaces by the DNA (or SNAREs) is likely to be the key. The linkers may affect the number of DNA that are able to hybridize between two vesicles, which could in turn affect the transition to fusion.

It is notable, then, that the T_{24} linker sequence is still able to mediate some degree of fusion when presented either on both partner vesicles or just one, showing that the presence of the linker does not prevent the reaction. In contrast, hybridization of only 5'-coupled DNA does not lead to fusion (22), even though after docking the spacing between these vesicles is comparable to that allowed by T_{24} linkers. For 5'-/3'-coupled linker DNA sequences, the expected geometry of docking, as well as the flexibility of single-stranded DNA [persistence length of only 1–3 nm (30, 32)] still allows for the close membrane contact thought to be necessary for fusion, while the duplex formed by 5'-coupled DNA may act as a stiff spacer between the vesicle surfaces.

For vesicles presenting a mixture of linker and nonlinker DNA (5'-α + 5'-$T_{24}\alpha$/3'-α' + 3'-$T_{24}\alpha'$, total $<n_{DNA}> = 100$), there are three different hybridization combinations possible: nonlinker–to–nonlinker, nonlinker–to–linker, and linker–to–linker. Of these, the first combination is most effective at driving fusion; thus, the second may sequester potentially fusogenic DNA into less-productive complexes, which would tend to reduce fusion kinetics. On the other hand, the enhancement in docking from the linker sequence expected for the latter two combinations would tend to increase fusion kinetics. Surprisingly, fusion kinetics are largely unchanged for vesicles presenting this mixture as compared to vesicles presenting only 5'-α/3'-α' (Fig. 5B and C, blue and red traces), which could indicate a balance between these competing effects, or could indicate the fusion is dominated by nonlinker DNA.

The experiments presented here illustrate the utility of DNA-mediated fusion as a model system, especially using the single-lipid anchor which avoids many of the complexities inherent in a double-anchored system as presented by Stengel et al. (23). Their system involves vesicle partners which each contain two prehybridized cholesterol-anchored DNA of differing lengths (23 and 15 bases). In this case, each vesicle presents a 15-base pair DNA duplex at the membrane proximal end, terminated by an 8-base ssDNA overhang in either a 5'- or 3'-orientation. They hypothesize, as we do, that initial hybridization of the overhang achieves 5'-/3'-docking, then duplex formation continues toward the membrane proximal bases in a "zippering" fashion, displacing the 15-mer on both vesicles. While this may be correct, it is also possible that strand displacement is not required to achieve fusion, but rather that hybridization proceeds only up to the shorter DNA. In this scenario, the membrane proximal DNA would presumably be left to act as a spacer, which from our results would still allow lipid and content mixing. This mechanism eliminates the need for a concerted, double-strand displacement of membrane-anchored strands, which is largely entropy-driven and, therefore, likely to be more difficult than strand displacement for nonanchored DNA (33). Also, this mechanism does not necessitate the intermediate formation—after strand displacement and before lipid mixing—of singly cholesterol–anchored DNA, which has been shown to partition unstably into lipid membranes and would, therefore, be lost into solution.

Increasing linker lengths shows a clear effect in increasing docking but reducing fusion kinetics, as has been observed previously for SNARE-mediated fusion (29). The experiments presented show that docking is necessary but not sufficient to lead to either lipid or content mixing. While it is relatively straightforward to relate DNA hybridization and docking, the number of DNA involved and the role of DNA in driving fusion beyond docking are less clear. It may be that the initial binding of the DNA pays some of the entropic cost of bringing the two membranes together, making it more probable that thermal fluctuations (or other machinery in the case of biological fusion) can overcome the transition barriers in the fusion process. It is also possible that the DNA plays a more active role in overcoming the substantial activation barrier against fusion. To shed more light on the fusion mechanism, we are continuing to explore the possibility of varying DNA sequence using both natural and artificial bases (34) to tailor hybridization energetics and to add dye-labels to allow for the quantification of hybridized DNA by FRET. Single vesicle assays with tethered vesicles are expected to be particularly useful to distinguish the progression in the stages of fusion more clearly than experiments performed in bulk.

Materials and Methods

DNA Sequences. The new DNA-lipid synthesis method is shown in Fig. 4 and is described more extensively in ref. 22. In brief, a lipid tailgroup-like glycerol derivative is converted into a phosphoramidite, which can be attached to any DNA sequence on conventional synthesizer to form the DNA-lipid conjugate. Experiments using different linker lengths all use the same 24-bp hybridization sequence (α and α'), but displaced from the membrane proximal end by $n = 0, 2, 4, 6, 12,$ or 24 T's ($T_n\alpha$ and $T_n\alpha'$). Table 1 lists all sequences, names, and DNA-coupling orientations used. Conjugates were all purified by high performance liquid chromatography (HPLC) and analyzed by matrix-assisted laser desorption/ionization time-of-flight (MALDI-TOF) mass spectrometry as described in ref. 22.

Vesicle Preparation. Dioleoylphosphatidylcholine (DOPC), dioleoylphosphatidyl-ethanolamine (DOPE), and cholesterol (Chol) were purchased from Avanti Polar Lipids. Texas Red-DHPE and Oregon Green-DHPE were purchased from Invitrogen. All lipids were used as received.

Vesicles displaying DNA were formed using a base lipid mixture of 2:1:1 by mole ratio of DOPC:DOPE:Chol. For lipid mixing experiments, one set of vesicles was made containing an additional 0.5 mol % TR-DHPE and 0.5 mol % OG-DHPE. Lipids were mixed in chloroform, dried under a nitrogen stream, then under vacuum, and resuspended in buffer solution to a concentration of 2 mg/ml. For lipid mixing experiments, the buffer was 10 mM Tris, pH 7.5 containing 100 mM sodium chloride. Two buffers were used for the partners in content mixing experiments: 10 mM Tris, pH 7.5 containing 8 mM terbium (III) chloride and 60 mM sodium citrate or 10 mM Tris, pH 7.5 containing 80 mM dipicolinic acid (DPA). After rehydration, lipids were extruded through a polycarbonate membrane (Whatman, pore size 50 nm) to form unilamellar vesicles. The concentration of vesicles in the resulting stock solutions is calculated to be roughly 0.11 μM in 50-nm vesicles. The mean of diameters was measured by dynamic light scattering to be 70–100 nm with a polydispersity between 0.05 and 0.1. DNA-lipid conjugates were typically dissolved in a 1:1 mixture of acetonitrile:water to form 100-μM stocks as calculated from the measured absorbance at 260 nm and extinction coefficient obtained from the SciTools utility from Integrated DNA Technologies. The appropriate amounts of DNA-lipid stock were added to the vesicle stocks (typically 2.8 μl to 50 μl, respectively) to achieve an average copy number of 50 DNA-lipids per vesicle. Although the DNA-lipid conjugates are soluble in 1:1 acetonitrile:water, they quantitatively partition into a vesicle (or supported membrane) bilayer (17). This has been demonstrated by patterning different DNA-lipid conjugate sequences on supported bilayers and demonstrating that mixtures of vesicles displaying the anti-sense sequence are selectively bound as expected by hybridization. Once bound, tethered vesicles do not leave the surface and

they can be moved around by electrophoresis and hydrodynamic flow without coming off the surface as long as the concentration of NaCl is above roughly 50 mM. Also, because of the order of addition and assembly process, the DNA is entirely on the outside of vesicles. After an overnight incubation at 4°C, all DNA-labeled vesicle aliquots were passed through a CL-4B size exclusion column (Sigma) equilibrated with 10 mM Tris buffer, pH 7.5 containing 100 mM sodium chloride for purification, and, in the case of content mixing experiments, removal of external TbCl$_3$ and dipicolinic acid. Lipid concentration after purification was characterized by an enzymatic assay for choline (35).

Docking Assays. A modification of the assay described in (5) was used to estimate the extent of vesicle docking. Vesicles were prepared as described for lipid mixing assays, except that one population was labeled with 0.5 mol % TR-DHPE and another with 0.5 mol % OG-DHPE. Vesicles presenting on average 50 copies of 5'-α/3'- α' or 5'-T$_{24}$α/3'-T$_{24}$α' were allowed to react under conditions identical to the fusion assay. Then an aliquot from the reaction mixture was diluted at various time points to a lipid concentration of 83 ng/ml, then injected into a CoverWell perfusion chamber gasket (9 mm diameter, 0.5 mm thickness, Molecular Probes) attached to a cleaned glass substrate. After 10 min, the vesicle solution was washed out with buffer and the adsorbed vesicles observed with a Nikon TE300 inverted epifluorescence microscope using a 100× oil immersion objective. The adsorbed vesicle surface density was ≈0.01 vesicles per μm². Docking was determined by overlaying the green and red images and counting the number of colocalized spots.

Fusion Assays. Lipid and content mixing assays were all performed at room temperature (25°C). The extent of lipid mixing was determined based on the dilution of OG and TR leaflet labels, which constitute a fluorescence resonance energy transfer (FRET) pair. After mixing the reacting vesicles in a cuvette to a final lipid concentration of 0.05 mg/ml (roughly 2.8 nM in vesicles assuming 50 nm diameter), emission spectra were taken at various times on a spectrofluorometer (SPEX, Horiba Jobin Yvon) using 488 nm excitation light. The FRET ratio was calculated as the emission intensity at 610 nm (TR acceptor) divided by the intensity at 530 nm (OG donor). After the timecourse was complete, the vesicles were disrupted by the addition of Triton-X to 0.2%, and the emission intensities were remeasured and used to normalize the FRET ratios (36). A standard curve to determine the extent of lipid mixing was constructed by plotting the normalized inverse FRET ratio (donor/acceptor fluorescence) for vesicles with 0.1, 0.25, 0.3, 0.4, 0.5, and 0.6 mol % of both OG and TR versus lipid/probe ratio. The data were well fitted by a linear equation, which was used to determine the effective concentrations of the leaflet labels at any given time point in the kinetics run. Because labeled and unlabeled vesicles are mixed at equal amounts, the extent of lipid mixing was calculated assuming that for a binary reaction, the effective dye concentration in both leaflets of the vesicles at completion should be half their starting concentration.

The extent of content mixing was determined by separately incorporating TbCl$_3$ and DPA into the contents of the two vesicle populations during extrusion. Content exchange between vesicles allows the formation of a fluorescent Tb(DPA)$_3^{3+}$ complex, whose emission intensity was measured at 490 nm upon excitation at 278 nm. To prevent false fusion signal from content leakage, 1 mM EDTA was included in the external reaction buffer to sequester any Tb^{3+} that had leaked out of the vesicles (22). Percent content mixing was estimated by comparison to vesicles containing a 1:1 mixture of the Tb and DPA buffers.

1. Chen YA, Scheller RH (2001) SNARE-mediated membrane fusion. *Nat Rev Mol Cell Biol* 2:98–106.
2. Jahn R, Lang T, Südhof TC (2003) Membrane fusion. *Cell* 112:519–533.
3. Brunger AT (2005) Structure and function of SNARE and SNARE-interacting proteins. *Q Rev Biophys* 38:1–47.
4. Weber T, *et al.* (1998) SNAREpins: Minimal machinery for membrane fusion. *Cell* 92:759–772.
5. Schuette CG, *et al.* (2004) Determinants of liposome fusion mediated by synaptic SNARE proteins. *Proc Natl Acad Sci US* 101:2858–2863.
6. Dennison SM, Bowen ME, Brunger AT, Lentz BR (2006) Neuronal SNAREs do not trigger fusion between synthetic membranes but do promote PEG-mediated membrane fusion. *Biophys J* 90:1661–1675.
7. Chen XC, Araç D, Wang T-M, Gilpin CJ, Zimmerberg J, Rizo J (2006) SNARE-mediated lipid mixing depends on the physical state of the vesicles. *Biophys J* 90:2062–2074.
8. Fix M, *et al.* (2004) Imaging single membrane fusion events mediated by SNARE proteins. *Proc Natl Acad Sci US* 101:7311–7316.
9. Bowen ME, Weninger K, Brunger AT, Chu S (2004) Single molecule observation of liposome-bilayer fusion thermally induced by soluble N-ethyl maleimide sensitive-factor attachment protein receptor (SNAREs). *Biophys J* 87:3569–3584.
10. Liu TT, Tucker WC, Bhalla A, Chapman ER, Weisshaar JC (2005) SNARE-driven, 25 millisecond vesicle fusion in vitro. *Biophys J* 89:2458–2472.
11. Yoon T-Y, Okumus B, Zhang F, Shin Y-K, Ha T (2006) Multiple intermediates in SNARE-induced membrane fusion. *Proc Natl Acad Sci USA* 103:19731–19736.
12. Li F, *et al.* (2007) Energetics and dynamics of SNARE-pin folding across lipid bilayers. *Nat Struct Mol Biol* 14:890–896.
13. Sutton RB, Fasshauer D, Jahn R, Brunger AT (1998) Crystal structure of a SNARE complex involved in synaptic exocytosis at 2.4 angstrom resolution. *Nature* 395:347–353.
14. Haque ME, McIntosh TJ, Lentz BR (2001) Influence of lipid composition on physical properties and PEG-mediated fusion of curved and uncurved model membrane vesicles: ''Nature's own'' fusogenic lipid bilayer. *Biochemistry* 40:4340–4348.
15. Gong Y, Ma M, Luo Y, Bong D (2008) Functional determinants of a synthetic vesicle fusion system. *J Am Chem Soc* 130:6196–6205.
16. Yoshina-Ishii C, Boxer SG (2003) Arrays of mobile tethered vesicles on supported lipid bilayers. *J Am Chem Soc* 125:3696–3697.
17. Yoshina-Ishii C, Miller GP, Kraft ML, Kool ET, Boxer SG (2005) General method for modification of liposomes for encoded assembly on supported bilayers. *J Am Chem Soc* 127:1356–1357.
18. Pfeiffer I, Höök F (2004) Bivalent cholesterol-based coupling of oligonucleotides to membrane assemblies. *J Am Chem Soc* 126:10224–10225.
19. Yoshina-Ishii C, *et al.* (2006) Diffusive dynamics of vesicles tethered to a fluid supported bilayer by single-particle tracking. *Langmuir* 22:5682–5689.
20. Yoshina-Ishii C, Boxer SG (2006) Controlling two-dimensional tethered vesicle motion using an electric field: Interplay of electrophoresis and electro-osmosis. *Langmuir* 22:2384–2391.
21. Chan Y-HM, Lenz P, Boxer SG (2007) Kinetics of DNA-mediated docking reactions between vesicles tethered to supported lipid bilayers. *Proc Natl Acad Sci USA* 104:18913–18918.
22. Chan Y-HM, van Lengerich B, Boxer SG (2008) Lipid-anchored DNA mediates vesicle fusion as observed by lipid and content mixing. *Biointerphases* 3:FA17-FA21.
23. Stengel G, Zahn R, Höök F (2007) DNA-induced programmable fusion of phospholipid vesicles. *J Am Chem Soc* 129:9584–9585.
24. Stengel G, Simonsson L, Campbell RA, Höök F (2008) Determinants for membrane fusion induced by cholesterol-modified DNA zippers. *J Phys Chem B* 112:8264–8274.
25. Boutorine AS, *et al.* (1989) Synthesis of alkylating oligonucleotide derivatives containing cholesterol or phenazinium residues at their 3'-terminus and their interaction with DNA within mammalian cells. *FEBS Lett* 254:129–132.
26. Haque ME, Lentz BR (2004) Roles of curvature and hydrophobic interstice energy in fusion: Studies of lipid perturbant effects. *Biochemistry* 43:3507–3517.
27. Siegel DP (2006) The modified stalk mechanism of lamellar/inverted phase transitions and its implications for membrane fusion. *Biophys J* 76:291–313.
28. Kasson PM, *et al.* (2006) Ensemble molecular dynamics yields submillisecond kinetics and intermediates of membrane fusion. *Proc Natl Acad Sci USA* 103:11916–11921.
29. McNew JA, Weber T, Engelman DM, Söllner TH, Rothman JE (1999) The length of the flexible SNAREpin juxtamembrane region is a critical determinant of SNARE-dependent fusion. *Mol Cell* 4:415–421.
30. Mills JB, Vacano E, Hagerman PJ (1999) Flexibility of single-stranded DNA: use of gapped duplex helices to determine the persistence lengths of Poly(dT) and Poly(dA). *J Mol Bio* 285:245–257.
31. Pobbati AV, Stein A, Fasshauer D (2006) N- to C-terminal SNARE complex assembly promotes rapid membrane fusion. *Science* 313:673–676.
32. Tinland B, Pluen A, Sturm J, Weill G (1997) Persistence length of single-stranded DNA. *Macromolecules* 30:5763–5765.
33. Letsinger RL, Chaturvedi SK, Farooqui F, Salunkhe M (1993) Use of hydrophobic substituents in controlling self-assembly of oligonucleotides. *J Am Chem Soc* 115:7535–7536.
34. Krueger AT, Lu H, Lee AHF, Kool ET (2007) Synthesis and properties of size-expanded DNAs: Toward designed, functional genetic systems. *Acc Chem Res* 40:141–150.
35. Nanjee MN, Gebre AK, Miller NE (1991) Enzymatic fluorometric procedure for phospholipid quantification with an automated microtiter plate fluorometer. *Clin Chem* 37:868–874.
36. Malinin VS, Haque ME, Lentz BR (2001) The rate of lipid transfer during fusion depends on the structure of fluorescent lipid probes: A new chain-labeled lipid transfer probe pair. *Biochemistry* 40:8292–8299.

Chan *et al.*